

## Deletions of Endocytic Components *VPS28* and *VPS32* Affect Growth at Alkaline pH and Virulence through both *RIM101*-Dependent and *RIM101*-Independent Pathways in *Candida albicans*

Muriel Cornet,<sup>1,2†</sup> Frédérique Bidard,<sup>1†</sup> Patrick Schwarz,<sup>3</sup> Grégory Da Costa,<sup>1</sup>  
Sylvie Blanchin-Roland,<sup>1</sup> Françoise Dromer,<sup>3</sup> and Claude Gaillardin<sup>1\*</sup>

Microbiologie et Génétique Moléculaire, Institut National Agronomique Paris-Grignon and Institut National de la Recherche Agronomique UMR1238, Centre National de la Recherche Scientifique UMR2585, 78850 Thiverval-Grignon, France<sup>1</sup>; Microbiologie, Hôtel-Dieu, 1 place du parvis Notre-Dame, 75181 Paris Cedex 04, France<sup>2</sup>; and Unité de Mycologie Moléculaire, CNRS FRE2849, Institut Pasteur, 25 rue du Dr. Roux, 75724 Paris Cedex 15, France<sup>3</sup>

Received 26 April 2005/Returned for modification 31 May 2005/Accepted 7 September 2005

**Ambient pH signaling involves a cascade of conserved Rim or Pal products in ascomycetous yeasts or filamentous fungi, respectively. Recent evidences in the fungi *Aspergillus nidulans*, *Saccharomyces cerevisiae*, *Yarrowia lipolytica*, and *Candida albicans* suggested that components of endosomal sorting complexes required for transport (ESCRT) involved in endocytic trafficking were needed for signal transduction along the Rim pathway. In this study, we confirm these findings with *C. albicans* and show that Vps28p (ESCRT-I) and Vps32p/Snf7p (ESCRT-III) are required for the transcriptional regulation of known targets of the Rim pathway, such as the *PHR1* and *PHR2* genes encoding cell surface proteins, which are expressed at alkaline and acidic pH, respectively. We additionally show that deletion of these two *VPS* genes, particularly *VPS32*, has a more drastic effect than a *RIM101* deletion on growth at alkaline pH and that this effect is only partially suppressed by expression of a constitutively active form of Rim101p. Finally, in an in vivo mouse model, both *vps* null mutants were significantly less virulent than a *rim101* mutant, suggesting that *VPS28* and *VPS32* gene products affect virulence both through Rim-dependent and Rim-independent pathways.**

*Candida albicans* is an opportunistic fungal pathogen that causes infections ranging from mucocutaneous illnesses to invasive processes that may involve any organ. The development of new therapies such as intensive chemotherapy for cancer or immunosuppressive regimens for transplantations, the increasing use of indwelling catheters and prosthetic devices, and progress in the treatment of bacterial infections have led to an increase in susceptible patients and cases of invasive *Candida* infections (12). The ability of *C. albicans* to colonize a wide range of tissues requires its adaptation to various environmental conditions, involving detection by the fungus of a variety of ambient signals. Extracellular pH is one of the environmental factors that modifies the physiology and morphology of the cell, and mutations in genes responding to external pH have been shown to result in less-virulent strains. For example, the cell wall protein Phr1p is expressed at a pH of  $\geq 5.5$  and is required for systemic candidiasis (blood pH is near neutrality), whereas its paralogue Phr2p is expressed only at acidic pH (pH  $\leq 5$ ) and is required for vaginal candidiasis (vaginal pH is around 4.5) (11, 19, 34).

A conserved fungal ambient pH signal transduction pathway was initially described for *Aspergillus* and was later extended to several ascomycetes, including *C. albicans* (9, 10, 13, 16, 30, 31). At alkaline pH, a cascade of six *Pal* genes in *Aspergillus nidulans* or five *RIM* genes in *Saccharomyces cerevisiae* acti-

vates the zinc finger transcriptional factor PacC/Rim101p through a C-terminal proteolytic processing event. This PacC/Rim101p short active form is able to activate alkaline pH-responsive genes and to repress acidic genes (15, 29, 35). Defects in this pathway lead to reduced virulence in *C. albicans*, *A. nidulans*, and other pathogenic fungi (5, 7–9, 17).

Recent observations made by several groups pointed out a possible contribution of vacuolar protein sorting (*VPS*) genes, encoding class E factors of the endocytic pathway, to the Rim-dependent pathway of pH signaling. In *S. cerevisiae*, genome-wide two-hybrid screens revealed that Rim13p and Rim20p interacted with Snf7p/Vps32p (named Vps32p in this paper) and that Rim20p interacted with Vps4p (6, 21). Vps32p forms part of the endosomal sorting complex required for transport (ESCRT) III (2), which acts downstream of ESCRT-I and ESCRT-II complexes in the multivesicular body (MVB) pathway, whereas the Vps4p AAA ATPase acts at the end of the endocytic cycle to dissociate ESCRT complexes from the endosomal membrane (3). In addition, both Vps32p and Vps4p were shown to interact with Bro1p/Vps31p (18), another soluble class E factor associated with endosomes and required for carboxypeptidase S sorting by the MVB pathway (28). The MVB pathway is conserved from yeast to higher eukaryotes and is required for a growing list of cellular functions that includes cell surface receptors and transporters degradation, regulation of the immune response, and even budding of certain viruses like human immunodeficiency virus (for reviews, see references 1 and 23).

Direct evidence for MVB class E factor involvement in ambient pH signaling was recently obtained for *Yarrowia lipolytica* (20; S. Blanchin-Roland et al., unpublished data), *S. cerevisiae*,

\* Corresponding author. Mailing address: Laboratoire de Microbiologie et Génétique Moléculaire, INRA, CBAI, 78850 Thiverval-Grignon, France. Phone: 33 1 30 81 54 52. Fax: 33 1 30 81 54 57. E-mail: claudie.gaillardin@grignon.inra.fr.

† Both authors contributed equally to this work.

TABLE 1. Strains used in this study

<i>Candida albicans</i> strain	Genotype				Reference or source
BWP17	<i>ura3Δ::λimm434</i>	<i>his1::hisG</i>	<i>arg4::hisG</i>		38
	<i>ura3Δ::λimm434</i>	<i>his1::hisG</i>	<i>arg4::hisG</i>		
DAY5	<i>ura3Δ::λimm434</i>	<i>his1::hisG</i>	<i>arg4::hisG</i>	<i>rim101::ARG4</i>	38
	<i>ura3Δ::λimm434</i>	<i>his1::hisG</i>	<i>arg4::hisG</i>	<i>rim101::URA3</i>	
DAY25	<i>ura3Δ::λimm434</i>	<i>pHIS1::his1::hisG</i>	<i>arg4::hisG</i>	<i>rim101::ARG4</i>	9
	<i>ura3Δ::λimm434</i>	<i>his1::hisG</i>	<i>arg4::hisG</i>	<i>rim101::URA3</i>	
DAY185	<i>ura3Δ::λimm434</i>	<i>pHIS1::his1::hisG</i>	<i>pARG4::URA3::arg4::hisG</i>		9
	<i>ura3Δ::λimm434</i>	<i>his1::hisG</i>	<i>arg4::hisG</i>		
MC1	<i>ura3Δ::λimm434</i>	<i>his1::hisG</i>	<i>arg4::hisG</i>	<i>vps28Δ::UAU1</i>	This study
	<i>ura3Δ::λimm434</i>	<i>his1::hisG</i>	<i>arg4::hisG</i>	<i>VPS28</i>	
MC2	<i>ura3Δ::λimm434</i>	<i>his1::hisG</i>	<i>arg4::hisG</i>	<i>vps28Δ::UAU1</i>	This study
	<i>ura3Δ::λimm434</i>	<i>his1::hisG</i>	<i>arg4::hisG</i>	<i>vps28Δ::URA3</i>	
MC3	<i>ura3Δ::λimm434</i>	<i>his1::hisG</i>	<i>arg4::hisG</i>	<i>vps32Δ::UAU1</i>	This study
	<i>ura3Δ::λimm434</i>	<i>his1::hisG</i>	<i>arg4::hisG</i>	<i>VPS32</i>	
MC4	<i>ura3Δ::λimm434</i>	<i>his1::hisG</i>	<i>arg4::hisG</i>	<i>vps32Δ::UAU1</i>	This study
	<i>ura3Δ::λimm434</i>	<i>his1::hisG</i>	<i>arg4::hisG</i>	<i>vps32Δ::URA3</i>	
MC2H	<i>ura3Δ::λimm434</i>	<i>pHIS1::his1::hisG</i>	<i>arg4::hisG</i>	<i>vps28Δ::UAU1</i>	This study
	<i>ura3Δ::λimm434</i>	<i>his1::hisG</i>	<i>arg4::hisG</i>	<i>vps28Δ::URA3</i>	
MC4H	<i>ura3Δ::λimm434</i>	<i>pHIS1::his1::hisG</i>	<i>arg4::hisG</i>	<i>vps32Δ::UAU1</i>	This study
	<i>ura3Δ::λimm434</i>	<i>his1::hisG</i>	<i>arg4::hisG</i>	<i>vps32Δ::URA3</i>	
MC5	<i>ura3Δ::λimm434</i>	<i>pVPS28::HIS1::his1::hisG</i>	<i>arg4::hisG</i>	<i>vps28Δ::UAU1</i>	This study
	<i>ura3Δ::λimm434</i>	<i>his1::hisG</i>	<i>arg4::hisG</i>	<i>vps28Δ::URA3</i>	
MC6	<i>ura3Δ::λimm434</i>	<i>pVPS32::HIS1::his1::hisG</i>	<i>arg4::hisG</i>	<i>vps32Δ::UAU1</i>	This study
	<i>ura3Δ::λimm434</i>	<i>his1::hisG</i>	<i>arg4::hisG</i>	<i>vps32Δ::URA3</i>	
MC13	<i>ura3Δ::λimm434</i>	<i>pRIM101SL::HIS1'rim101</i>	<i>arg4::hisG</i>	<i>rim101::ARG4</i>	This study
	<i>ura3Δ::λimm434</i>	<i>RIM101</i>	<i>arg4::hisG</i>	<i>rim101::URA3</i>	
MC14	<i>ura3Δ::λimm434</i>	<i>pRIM101SL::HIS1'rim101</i>	<i>arg4::hisG</i>	<i>vps28Δ::UAU1</i>	This study
	<i>ura3Δ::λimm434</i>	<i>RIM101</i>	<i>arg4::hisG</i>	<i>vps28Δ::URA3</i>	
MC15	<i>ura3Δ::λimm434</i>	<i>pRIM101SL::HIS1'rim101</i>	<i>arg4::hisG</i>	<i>vps32Δ::UAU1</i>	This study
	<i>ura3Δ::λimm434</i>	<i>RIM101</i>	<i>arg4::hisG</i>	<i>vps32Δ::URA3</i>	

and *C. albicans* (24, 39). Current models suggest that ESCRT complexes, mainly through their Vps32p moiety, function at neutral and/or alkaline pH as an assembly platform for the recruitment of Rim components leading to Rim101p activation (24, 29, 39). In this paper, we confirm the above conclusions and show that *VPS* genes may play additional roles in the control of the alkaline response and that *vps* deletions result in more pronounced defects in pathogenesis than would be expected with a simple interruption of the Rim pathway.

#### MATERIALS AND METHODS

**Strains and sequence data.** The bacterial strain used for transformation and amplification of recombinant DNA was *Escherichia coli* DH5α. *C. albicans* strains are described in Table 1. All *C. albicans* sequence data were obtained from <http://genolist.pasteur.fr/CandidaDB/>.

**Culture media and phenotypic tests.** For gene expression experiments, synthetic complete medium (SC) was used, consisting of a 0.67% yeast nitrogen base, 2% glucose, and 0.77-g/liter complete amino acid supplement mixture without arginine and histidine, supplemented when required with uridine (Uri; 80 μg/ml), arginine (20 μg/ml), and histidine (20 μg/ml). Growth experiments at various pHs were carried out in SC (pH 5.3) and in SC buffered with 50 mM glycine-NaOH at either pH 9.0 or pH 10.0 and with 0.2 M citrate phosphate at

pH 3.0. Droplets of serial dilutions of an exponential-phase culture in yeast extract-peptone-glucose (YPD) medium were spotted on SC, SC (pH 3.0), SC (pH 9.0), or SC (pH 10.0) and incubated at 30°C. For the filamentation assays, we used M199 medium (Invitrogen, Paisley, United Kingdom) buffered at pH 4.0 or pH 7.5 with 150 mM HEPES as previously described (10). Data were averaged from three independent experiments. As the reference strain cells produce hyphae extensively at 37°C and pH 7.5, growth rates under these conditions in both SC and M199 media were determined by dry weight measurements as follows. Cells were grown overnight in SC medium, diluted in 100 ml SC or M199 (pH 7.5) to an optical density at 600 nm (OD<sub>600</sub>) of about 0.1, and grown at 37°C. Every 2 h, 5 ml of the culture was filtered through glass microfiber filters (Whatman, Maidstone, United Kingdom) that were predried at 80°C overnight and preweighed. Then the filters were dried at 80°C overnight, and dry weights were calculated.

**DNA and RNA techniques.** Standard recombinant DNA techniques were performed as previously described (32). All transformation events were checked by colony PCR using puRE Taq Ready-To-Go PCR Beads (Amersham, Piscataway, NJ) and confirmed by Southern blot analysis. Sequences were obtained from the DNA sequencing department of Eurogentec (Ivoz-Ramet, Belgium). They were assembled and annotated with the Genetics Computer Group package (Madison, WI).

Gene expression was determined by quantitative real-time PCR using a light cycler (Roche Molecular Biochemicals, Meylan, France). Cells were grown in SC buffered at pH 4.0 or pH 7.5 with 150 mM HEPES at 30°C and harvested in the exponential phase (OD<sub>600</sub>, ~0.6). Cells were pelleted, frozen in liquid nitrogen,

TABLE 2. List of primers used in this study

Oligonucleotide	Sequence (5' to 3')
OFB3.....	GTTCATCCTTAGTCATAGAACAACTTTGATTATTGTCATTATGACGCTTCGCCCTGTGGAATTGTGAGCG
OFB4.....	CGAATCCATCGTATAAGCAAGAAACAGAGTATCCAACCAACAGATAATTGTTATTGTGTTTCCAGTCACGAC
OFB5.....	CTTTAGTTGACTGAATAAACTTGAATAGTAAACATGTGGGGATATTTTTTGGAGGAAATGTGGAATTGTGAGCG
OFB6.....	TTCTATACAAAGCTTTCGTTATCTCCGTAATTCGGTATTTCAACACATCATAATCCCATTTGTTTCCAGTCACGA
OFB8.....	AATTCACACATCGTAAATCGAAC
OFB9.....	ACCAATGTTGATAACCAATCGGT
OFB10.....	CATCATCCCGGAAATACATCCA
OFB11.....	TACGTTATTTGAATGTGTGTTATCA
OFB16.....	TGTGACGACCATGTTGGTAGAAAGT
OFB17.....	CTTGAGGTCTCTTGAACGATTGCG
OFB22.....	GCAGTGCTTCAATCAATAGCAAGGC
OFB23.....	AGAGCTTGAGCTGGACCCAGA
OFB32.....	AGTGTGACATGGATGTTAGAAAAGAATTATACGG
OFB33.....	ACAGAGTATTTCTTTCTGGTGGAGCA
OFB40.....	ACACTGACGCTTCTGCTTTCG
OFB41.....	GCAGCTTCGTCTTCATCACCACA
OFB48.....	ACTCTAGCCGCGGTACCAAG
OFB50.....	ACATAGGCTCTCCGTATAGAC
OFB57.....	CCACAAGAAATGTCCGATGC
OFB58.....	TCCATGTTCCACTGCCTCAG
OFB59.....	GCCACTATGGTGAGCGAACA
OFB60.....	GACACTTCTGTTGCAAGGTG
OMC15.....	GCTACTAGGGTCACTGCAAAATCG
OMC16.....	CTAGAAGCGCTAGATGAAGTAC
OMC7.....	GGTGGTGTCTTCTGCTATTAAAC
OMC8.....	CCAGTTGCAATTGCTTGACCG
OMC9.....	CTCTCGTCTCTATCTGTCAGTGG
OMC10.....	GTGTAGTATCCGTTGGTTCGTC
OMC11.....	GCGTTTGGCTCTTGTCTTTC
OMC12.....	CCAACCTGGCCATAAGAGCCTC

and kept at  $-80^{\circ}\text{C}$  until RNA isolation. Total RNA was extracted with the RNeasy Mini-kit (QIAGEN, Courtabouef, France) and then treated with DNase I (QIAGEN). The Superscript II RNase H-Reverse Transcriptase kit (Invitrogen) was used for a reverse transcriptase assay from 1  $\mu\text{g}$  of total RNA. The real-time PCR assay was performed using the following primer pairs: OFB16-OFB17 for *RIM101*, OFB22-OFB23 for *PHR1*, OFB32-OFB33 for *ACT1*, and OFB40-OFB41 for *PHR2* (primer sequences are shown in Table 2). PCR parameters were  $95^{\circ}\text{C}$  for 8 min, followed by 45 cycles, each consisting of  $95^{\circ}\text{C}$  for 10 s,  $55^{\circ}\text{C}$  for 7 s, and  $72^{\circ}\text{C}$  for 10 s. A negative control with sterile water was performed for each primer set. The threshold cycle was determined as the cycle above which the fluorescence signal, produced by the SYBRgreen I dye, reached a baseline level. The expression levels of the genes were determined relative to the expression of the *ACT1* gene. For each gene, experiments were carried out four times, using two cDNA samples from two independent cultures.

**Construction of strains.** Complete deletions of *VPS28* (*vps28*<sup>-/-</sup>; strain MC2) and *VPS32* (*vps32*<sup>-/-</sup>; strain MC4) were constructed by the UAU1 method (14) with the BWP17 strain (38). The UAU1 cassette was amplified from plasmid pBME101 (14) with primers OFB3-OFB4 for the *VPS28* gene and OFB5-OFB6 for the *VPS32* gene, using the Expand High Fidelity PCR System kit (Roche Molecular Biochemicals). These primers allow amplification of the UAU1 cassette with 60- and 61-nucleotide (nt)-long flanking sequence homologues to *VPS28* and *VPS32*, respectively. Transformants of the BWP17 strain obtained with the UAU1 cassette were screened by colony PCR: wild-type *VPS28* and *VPS32* alleles were detected using primers OFB8-OFB9 and OFB10-OFB11, respectively; mutant *vps28*::*UAU1* and *vps32*::*UAU1* alleles were detected using primer OFB8 or OFB10, respectively, with Arg4det (14). Among the nearly 100 transformants obtained for each gene, 5 of 16 (31%) and 3 of 74 (4%) tested by PCR were heterozygous clones *VPS28*<sup>+/+</sup> (MC1) and *VPS32*<sup>+/+</sup> (MC3), respectively. Five *vps28*<sup>-/-</sup> (MC2) and two *vps32*<sup>-/-</sup> (MC4) homozygotes were obtained from independent heterozygotes by mitotic recombination after growth on YPD medium at  $30^{\circ}\text{C}$  for 48 h and selected by replication onto SC medium without arginine and without Uri. Arg<sup>+</sup> Uri<sup>+</sup> colonies were screened by colony PCR, and integration was confirmed by Southern blot analysis.

To differentiate haplotypes in the *VPS28* and *VPS32* regions, we used the SCS314 genome assembly (<http://www.candidagenome.org/>). We aligned contig 9-10045 and contig 19-20045 on chromosome 2 for *CaVPS28*, and contigs 19-10237 and 19-20237 on chromosome 1 for *CaVPS32*. Both alleles of *CaVPS28*

and *CaVPS32* lie in 100% identical regions, flanked by regions where numerous insertions and deletions differentiate both haplotypes. Two oligonucleotides (Table 2) hybridizing in conserved regions were designed to amplify the right border of the *CaVPS28* haplotypes: OMC15 (nt 26453-26475 in contigs 19-10045 and 19-20045) and OMC16 (nt 29069 to 29047 in contig 19-10045 and nt 28363 to 28385 in contig 19-20045). Amplicons of 2,616 and 1,932 bp were predicted for each haplotype. Similarly, two primers, OMC7 (nt 53278 to 53299 in contig 19-10045 and nt 52589 to 52610 in contig 19-20045) and OMC8 (nt 53678 to 53658 in contig 19-10045 and nt 53106 to 53086 in contig 19-20045), were used to amplify the *CaVPS28* left border. Amplicon sizes of 400 and 520 bp were expected. In the case of *CaVPS32*, primers OMC9 (nt 57459 to 57480 in contig 19-10237 and nt 57512 to 57533 in contig 19-20237) and OMC10 (nt 58440 to 58419 in contig 19-10237 and nt 58435 to 58414 in contig 19-20237) were used for the left border; amplicons of 980 and 922 bp were expected. Primers OMC11 (nt 153337 to 153356 in contig 19-10237 and nt 153348 to 153367 in contig 19-20237) and OMC12 (nt 157452 to 157431 in contig 19-10237 and nt 153477 to 153456 in contig 19-20237) were used for the right border. Amplicons of 4,116 and 130 bp were expected.

Finally, pINA1337 (F. Bidard, unpublished data), a derivative of pFLAG-MET3 (36) and carrying the *HIS1* cassette and the *MET3* promoter, was linearized by *Sma*I and targeted into MC2 and MC4 at the *HIS1* locus to yield prototrophic strains MC2H and MC4H, respectively.

For complementation, the wild-type *VPS28* and *VPS32* genes were amplified from BWP17 genomic DNA with primers OFB57-OFB58 and OFB59-OFB60, respectively. For the *VPS28* gene, the resulting PCR product was inserted into pDDB78 carrying the *HIS1* cassette and digested with *Sma*I to construct pDO14 (26). The *VPS32* gene was first inserted into pGEM-T-Easy (Promega, Charbonnières, France) and then into pDDB78 digested with *Not*I to give pDO15. The absence of mutation in each open reading frame was checked by DNA sequencing. *Nru*I-digested pDO14 and pDO15 were targeted to the *HIS1* locus of MC2 and MC4, respectively, to construct the *vps28*<sup>-/-</sup>+*VPS28* (MC5) and *vps32*<sup>-/-</sup>+*VPS32* (MC6) strains. Correct integration was confirmed by Southern blot analysis for both complemented strains.

A C-terminal truncated form of *RIM101*, encoding a 415-residue protein, constitutively active, called Rim101SLp, was created by a G-to-T substitution at position 1246, thus creating an in frame amber codon (D. Onesime, unpublished data); all coordinates start at the ATG of the full-length open reading frame as

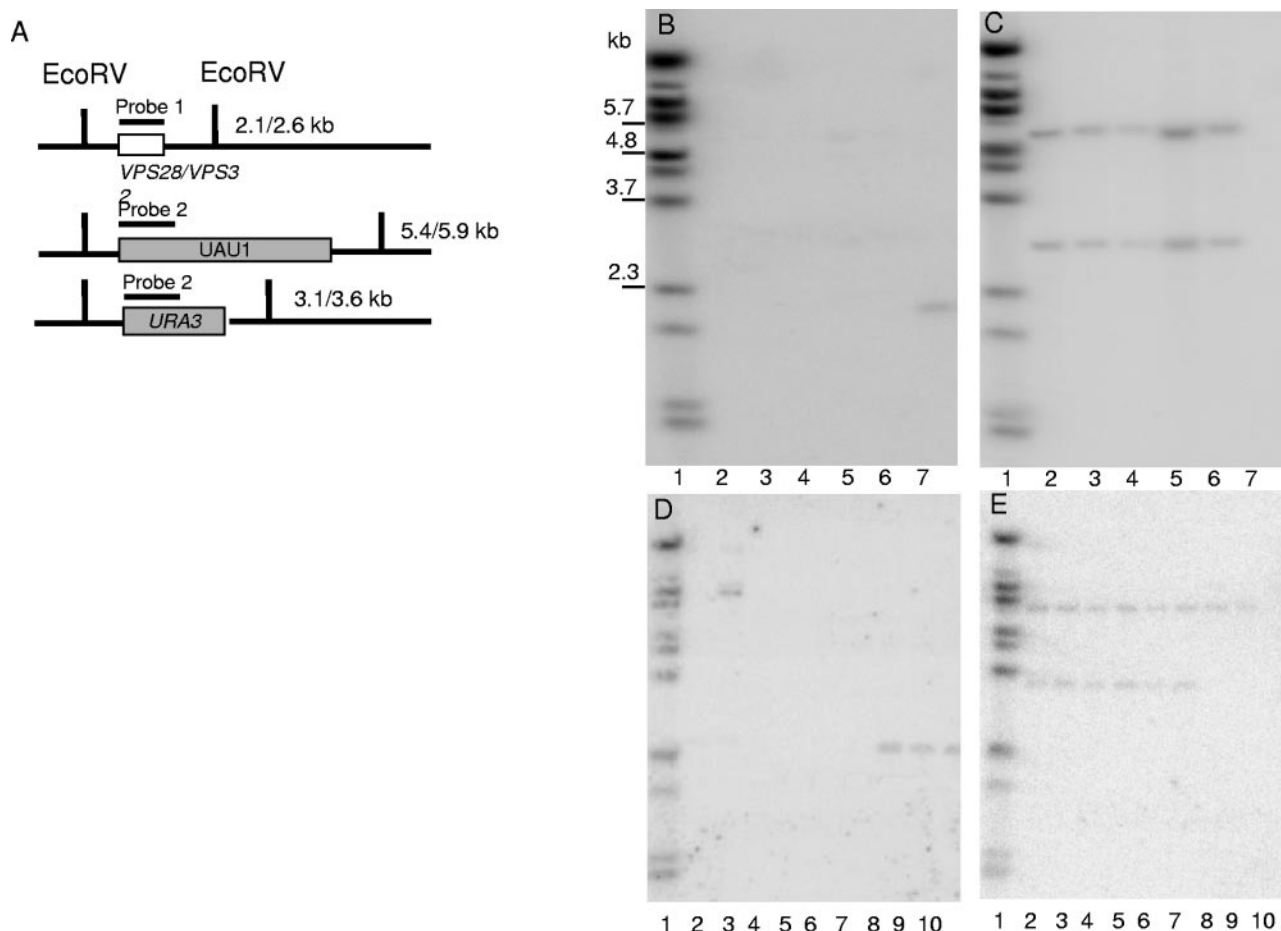


FIG. 1. Confirmation of the *vps* deletions by Southern analysis. (A) Schematic restriction map of the *VPS28* and *VPS32* wild-type and deleted alleles. Vertical bars denote EcoRV restriction sites, and numbers on their right indicate predicted sizes obtained with the *VPS28* or the *VPS32* probe (probe1) for the wild-type alleles and the *URA3* probe (probe 2 is a 0.8-kb *URA3* fragment obtained by XhoI and PvuII digestion of pBME101 (14) for the deleted alleles. (B and C) Southern blot analysis of EcoRV-digested genomic DNA from the five *vps28*<sup>-/-</sup> deleted strains (lanes 2 to 6) and the BWP17 parent strain (lane 7), using the *VPS28* probe (B) or the *URA3* probe (C). (D and E) Southern blot analysis of EcoRV-digested genomic DNA from six *vps32*<sup>-/-</sup> deleted strains (lanes 2 to 7), two heterozygote-deleted strains (lanes 8 and 9), and the BWP17 parent strain (lane 10), using the *VPS32* probe (D) or the *URA3* probe (E). Lanes 2 to 5 are double deletants obtained from the lane 8 heterozygote, whereas lanes 6 and 7 show double deletants obtained from the other heterozygote (lane 9). Lane 1 is a lambda DNA-BstEII digest marker for all panels.

defined previously (13). The truncation site was determined by hydrophobic cluster analysis as for the *YIRIM101-1119* allele (25). Plasmid pINA1353 was generated from plasmid pINA1341 (Bidard, unpublished), carrying *RIM101SL* under the control of the *MET3* promoter, by digestion with StuI and HpaI to remove the *MET3* promoter. PpuMI-digested pINA1353 was targeted to the *RIM101* locus of strains DAY5, MC2, and MC4, generating a tandem structure of *RIM101* genes which restored the wild-type 5' upstream sequence in front of *RIM101SL* and deleted the promoter of the resident *RIM101* copy. This resulted in strains MC13, MC14, and MC15, respectively. Integration was confirmed by colony PCR using primers OFB48-OFB50 and Southern blot analysis.

**Staining with FM4-64.** To analyze yeast vacuolar morphology and dynamics, FM4-64 localization experiments were performed with a protocol derived from Vida and Emr (37). Yeast cells were grown in YPD to an OD<sub>600</sub> of 0.5 to 0.7. Three OD units of cells were harvested, incubated in 150  $\mu$ l of YPD containing 40  $\mu$ M FM4-64 (Molecular Probes, Eugene, OR) for 30 min at 0°C, washed three times in phosphate-buffered saline at 0°C, and further incubated in 200  $\mu$ l of YPD for 20 min at 18°C. Cells were centrifuged, resuspended in water, and visualized by differential interference contrast (DIC) optics and by fluorescence microscopy using an Olympus U-RFL-T microscope equipped with a CoolSNAP camera.

**Virulence assay.** All strains were grown on Sabouraud agar and subcultured on YPD medium at 30°C for 24 h. Cells were harvested, washed twice in sterile

physiological saline, counted with a hemocytometer, and adjusted to  $2 \times 10^6$  or  $2 \times 10^7$  CFU/ml in sterile physiological saline. BALB/c male mice, 7 weeks old (Charles River, Les Oncins, France), were housed in groups of seven mice per cage and were inoculated by injection of 100  $\mu$ l with one of the above yeast suspensions into the lateral tail vein (final amount,  $2 \times 10^5$  or  $2 \times 10^6$  CFU per mouse). Dilutions of the suspensions were plated on Sabouraud agar to confirm the inoculum size. Survival was monitored twice daily until day 30 postinfection. The log rank test was used to determine significant differences in survival time between groups using GraphPad Prism 3.0 software (GraphPad, San Diego, CA). A *P* value of <0.05 was considered significant.

**Fungal burden and morphological analysis.** To assess fungal burden and morphology in infected tissues, a less acute infection was required. We therefore used an inoculum of  $5 \times 10^5$  CFU per mouse. Fungal cells were prepared and injected as described above. Five mice were infected with each strain and euthanized at day 4 postinfection. The kidneys being the target organs in this model (27), the left kidney was aseptically removed, weighed, and homogenized in 2 ml of sterile physiological saline; serial dilutions were plated on Sabouraud chloramphenicol agar for determination of the CFU per g of kidney. Statistical analysis was performed using the nonparametric Dunn's test for multiple comparisons. A *P* value of <0.05 was considered significant. Morphology of *C. albicans* cells recovered from infected kidneys was assessed using calcofluor white (Sigma, St. Quentin Fallavier, France) that stains chitin within the cell wall.

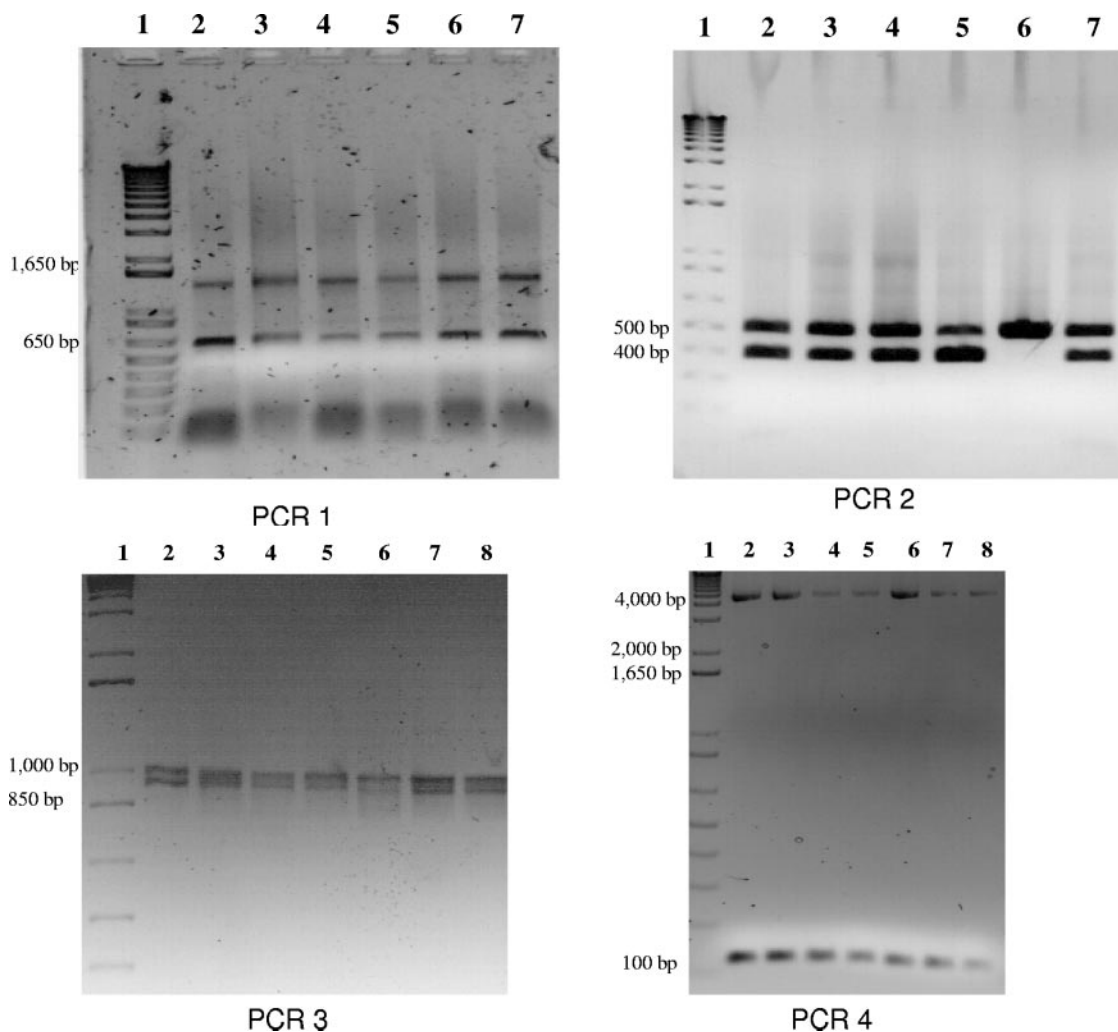


FIG. 2. PCR amplifications of the two haplotypes in heterozygous regions flanking *VPS28* and *VPS32*. (Top) Right and left borders of *VPS28* (PCR1 and PCR2, respectively). Lane 1, 1-kb Plus DNA ladder; lane 2, BWP17; lanes 3 and 4, two *VPS28*<sup>+/−</sup> single disruptants; lanes 5 to 7, three independent *vps28*<sup>−/−</sup> double disruptants. (Bottom) Left and right borders of *VPS32* (PCR3 and PCR4, respectively). Lane 1, 1-kb Plus DNA ladder; lane 2, BWP17; lanes 3 and 4, two *VPS32*<sup>+/−</sup> single disruptants; lanes 5 to 8, *vps32*<sup>−/−</sup> double disruptants (strains lanes 5 and 6 were obtained from the lane 3 single disruptant, and strains 7 and 8 were obtained from the other single disruptant).

Thus, 50  $\mu$ l of each kidney homogenate was stained with 10  $\mu$ l of a solution of 0.1% calcofluor white and 1% KOH. Slides were observed by fluorescence microscopy with a 340- to 380-nm filter and the same microscope as for FM4-64 staining. To quantitate the morphogenesis defects, we used the morphological index (MI) described previously by Odds et al. (27): cells were categorized as yeasts showing a spherical shape (MI score = 1), elongated yeasts showing ovoid shape and a length up to twice the diameter of the cell (MI score = 2), pseudohyphae (MI score = 3), or true hyphae (MI score = 4). For each stained homogenate, 50 cells were scored; data are the average of five mice infected with each strain. The nonparametric Kruskal-Wallis test was used for statistical analysis.

## RESULTS AND DISCUSSION

**Isolation of *vps* mutants.** Recently and while this work was in progress, studies with *S. cerevisiae* established that Rim101p processing was dependent on class E VPS factors belonging to the three ESCRT complexes required for sorting membrane proteins into the MVB pathway (39). Conservation of this process in *C. albicans* was assumed following the observations that class E *vps* mutants inhibit alkaline-induced filamentation

and that this inhibition is relieved by expression of a constitutively active form of Rim101p (39). A direct requirement of Vps32p for Rim101p processing in *C. albicans* was shown independently (24). To confirm this link in *C. albicans*, we checked the effects of the deletion of two *VPS* genes on the expression of alkaline and acidic genes and on the growth and hyphal development at various pHs.

The *VPS28* and *VPS32* genes were chosen as components of the ESCRT-I and ESCRT-III complexes, respectively (2, 22) and strains carrying heterozygous and homozygous null mutations in the BWP17 background were generated by the UAU1 method (14) (see Materials and Methods and Table 1). Confirmation of the *vps28* and *vps32* deletions by Southern analysis is shown in Fig. 1. The *vps32* homozygous mutant that exhibited an unexpected hybridization with the *VPS32* probe was not considered in this study (Fig. 1D, lane 3). This method involves spontaneous transfer of the disruption cassette from one chromosome to its homologue. We thus checked whether homog-

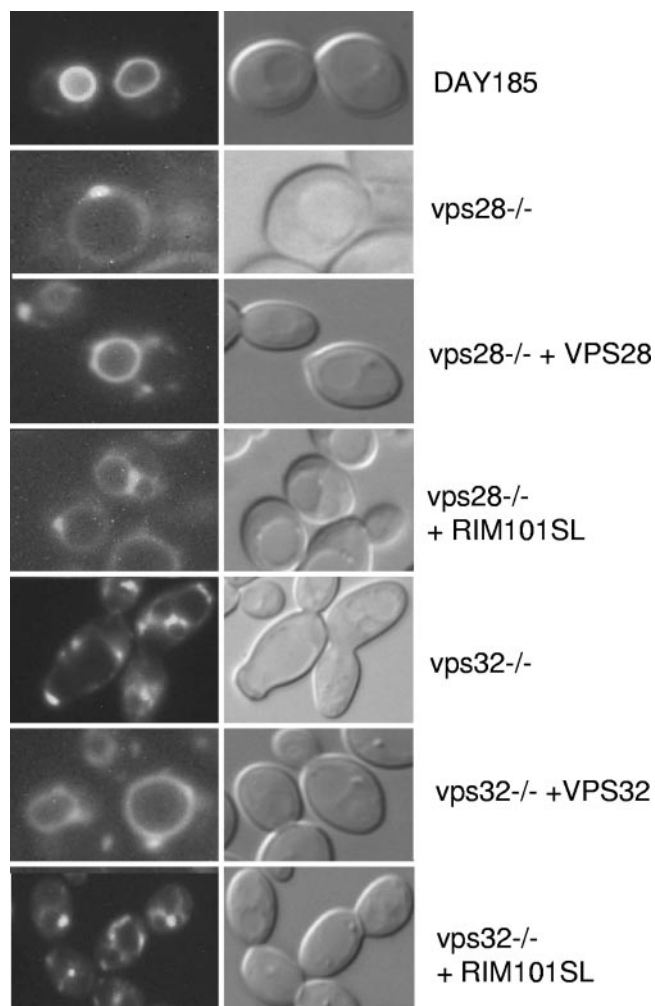


FIG. 3. FM4-64 staining in the *C. albicans* mutants. The strains were DAY185 (reference strain), MC2H (*vps28*<sup>-/-</sup>), MC5 (*vps28*<sup>-/-</sup> + *VPS28*), MC14 (*vps28*<sup>-/-</sup> + *RIM101SL*), MC4H (*vps32*<sup>-/-</sup>), MC6 (*vps32*<sup>-/-</sup> + *VPS32*), and MC15 (*vps32*<sup>-/-</sup> + *RIM101SL*). They were incubated with 40  $\mu$ M FM4-64 as described in Materials and Methods and visualized by fluorescence microscopy. The left side of each panel is FM4-64 fluorescence, while the right side of each panel shows differential interference contrast optics.

enotization of a large chromosomal segment occurred simultaneously. According to sequence data available for SC5314, the ancestor of the BWP17 strain used here (38), the *CaVPS28* and *CaVPS32* alleles lie in 24-kb and 96-kb homozygous regions of chromosome 2 and 1, respectively, flanked by heterozygous regions. The status of the flanking regions in the parental strain was checked by PCR (see Materials and Methods), as well as in the single and double disruptants. As shown on Fig. 2, lanes 2 to 4, and as expected, heterozygosity of the *VPS28* and *VPS32* flanking regions was conserved in BWP17 and in all single disruptants checked. Expected sizes of amplicons were observed, except in the case of the *VPS28* right border; this may reflect genomic variations between BWP17 and SC5314 generated during the successive transformations that lead to this strain (38). All double *CaVPS32* disruptants retained the chromosomal structure of the parental strain,

whereas one of the *CaVPS28* double disruptants lost heterozygosity at the left border (Fig. 2, panel PCR2, lane 6). This strain was discarded. Haplotypes initially present on chromosomes 1 and 2 were thus conserved, except for the 24- and 96-kb regions separating the heterozygous markers where extensive homogenization may have occurred. We therefore cannot rule out that some of the phenotypes displayed by our mutants may result from unmasking of preexisting or transformation-induced mutations in these regions. The fact that most phenotypes could be completely complemented by insertion of an ectopic copy of the wild type argues against such a hypothesis (see below).

FM4-64 localization experiments indicated that double disruptants for *CaVPS28* or *CaVPS32* displayed defects in endocytosis (24). Twenty minutes after being stained, FM4-64 dye could clearly be seen on the vacuole membrane in the reference strain (DAY185) cells, while it remained in small compartments adjacent to the vacuole in the two *vps* mutant cells (Fig. 3). These structures were highly reminiscent of class E compartments, which accumulate proteins destined for the vacuole in class E *vps* mutants in *S. cerevisiae* (33, 37). This phenotype was lost upon introduction of a wild-type copy of the disrupted alleles (Fig. 3).

**Role of the *VPS28* and *VPS32* genes in alkaline and acidic genes regulation.** The effects of *vps28* and *vps32* deletions on the transcription of the alkaline-induced genes (*RIM101* and *PHR1*) and of the acid-induced and alkaline-repressed gene *PHR2* were estimated by quantitative real-time PCR of transcripts extracted from cells grown at pH 4.0 and pH 7.5, using actin transcripts as a reference (Fig. 4).

In heterozygous *vps*-deleted strains *vps28*<sup>+/-</sup> and *vps32*<sup>+/-</sup> at pH 4.0 and pH 7.5, *RIM101*, *PHR1*, and *PHR2* expression levels were comparable to those observed for the reference strain (data not shown). In the *vps28*<sup>-/-</sup> and *vps32*<sup>-/-</sup> homozygous backgrounds and at pH 4.0, the *RIM101*, *PHR1*, and *PHR2* mRNA levels were not significantly affected (Fig. 4). At pH 7.5, both homozygous deletions of *VPS28* and *VPS32* significantly decreased *RIM101* expression and abolished *PHR1* expression, whereas *PHR2* expression derepressed up to twice its level at acidic pH in the reference strain. These effects are completely similar to those observed with the *rim101* homozygous deletion (Fig. 4). Complementation of the *vps28*<sup>-/-</sup> and *vps32*<sup>-/-</sup> homozygous deleted strains with one copy of their corresponding wild-type allele completely restored a wild-type phenotype.

These results confirm that Vps28p and Vps32p are required at alkaline pH for *PHR1* and *RIM101* induction and for *PHR2* repression, two processes known to require Rim101p activation. To further confirm this hypothesis, we checked whether expression of a constitutively active form of Rim101p was able to bypass the *vps* defects. To this end, we integrated a plasmid carrying *RIM101SL*, encoding a 415-residue C-terminally truncated form of Rim101p, in the various mutants at the *RIM101* locus (see Materials and Methods). Transcript levels of *RIM101SL* made under these conditions were similar to those driven by the native *RIM101* gene (compare *RIM101* expression in the reference strain and in the *rim101*<sup>-/-</sup> + *RIM101SL* backgrounds at pH 7.5) (Fig. 4). On the contrary, and as shown in Fig. 4, expression of *RIM101SL* in *vps* null mutants led to partial derepression

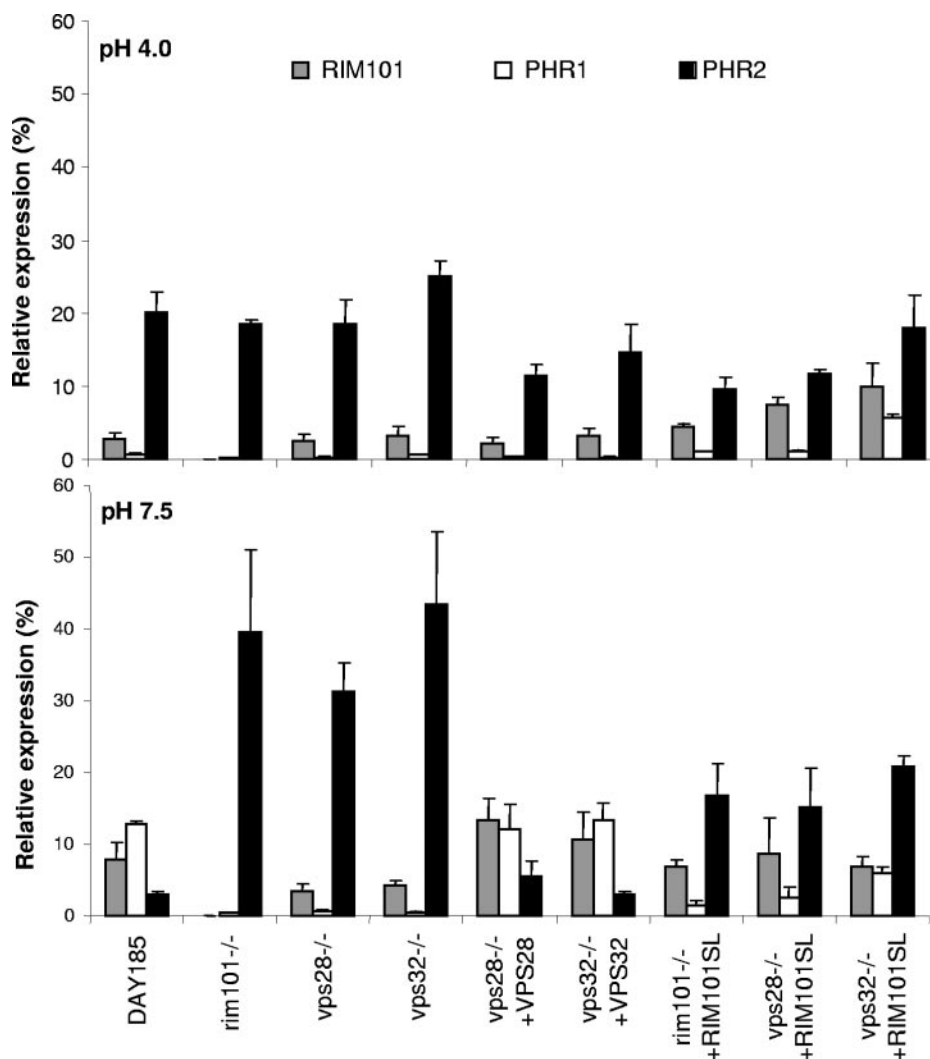


FIG. 4. Expression patterns of alkaline-induced genes (*RIM101* and *PHR1*) and acid-induced gene (*PHR2*) in *C. albicans* strains at pH 4.0 and pH 7.5. The strains were (from left to right) DAY185 (reference strain), DAY25 (*rim101*<sup>-/-</sup>), MC2H (*vps28*<sup>-/-</sup>), MC4H (*vps32*<sup>-/-</sup>), MC5 (*vps28*<sup>-/-</sup> + *VPS28*), MC6 (*vps32*<sup>-/-</sup> + *VPS32*), MC13 (*rim101*<sup>-/-</sup> + *RIM101SL*), MC14 (*vps28*<sup>-/-</sup> + *RIM101SL*), and MC15 (*vps32*<sup>-/-</sup> + *RIM101SL*). Expression levels were calculated relative to the expression of the *ACT1* reference gene. Data are the average of four experiments.

of *PHR1* and partial repression of *PHR2* at both pHs. These effects are qualitatively similar to those observed after the suppression of a *rim101* homozygous deletion (*rim101*<sup>-/-</sup> + *RIM101SL*) (Fig. 4); they suggest that our truncated allele does not perfectly mimic the physiologically active form of Rim101p and show that regulation of *PHR1* and *PHR2* is restored at alkaline pH in *vps* mutants to the same extent as it would be in a *rim* mutant. However, the suppression induced by the *RIM101SL* truncated form in the *vps* mutants, even partial, suggests that Vps28p and Vps32p act in the Rim pathway upstream from the processing of Rim101p. As the expression of this *RIM101SL* truncated allele has no effect on the endocytic phenotype (Fig. 3), the role of the two Vps factors in the Rim pathway appears separate from their role in the MVB transport machinery.

**Role of *VPS28* and *VPS32* on growth and morphology at acidic and alkaline pH.** On solid SC medium, two independent clones of each *vps28*<sup>-/-</sup> and *vps32*<sup>-/-</sup> homozygous deletion grew as well as the reference strain at pHs 3.0 and 5.3 (Fig. 5). At pH

9.0, the *vps32*<sup>-/-</sup> strain was affected more drastically than the *vps28*<sup>-/-</sup> and the *rim101*<sup>-/-</sup> null homozygotes that still showed a growth pattern near the reference strain. At pH 10.0, the *vps32*<sup>-/-</sup> strain was unable to form colonies, whereas both *vps28*<sup>-/-</sup> and *rim101*<sup>-/-</sup> were severely affected, with *vps28*<sup>-/-</sup> being slightly more sensitive than *rim101*<sup>-/-</sup>. Growth inhibition at alkaline pH was totally repaired after integration of one copy of the corresponding wild-type allele at the *HIS1* locus (*vps28*<sup>-/-</sup> + *VPS28* and *vps32*<sup>-/-</sup> + *VPS32*) (Fig. 5). The suppression by the constitutively active *RIM101SL* gene was nearly complete in the case of the *rim101*<sup>-/-</sup> + *RIM101SL* strain but only partial in strains *vps28*<sup>-/-</sup> + *RIM101SL* and *vps32*<sup>-/-</sup> + *RIM101SL*. This suppression by the *RIM101SL* gene was confirmed by growth experiments in liquid SC medium buffered at pH 9.0 (data not shown).

These results show that the VPS factors have a significant function in the alkaline response and suggest that this function is not only Rim dependent.

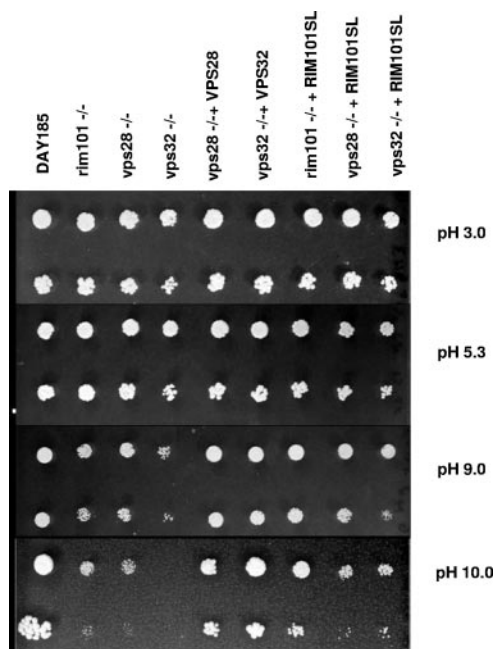


FIG. 5. Sensitivity of *C. albicans* strains to ambient pH. The strains were (from left to right) DAY185 (reference strain), DAY25 (*rim101*<sup>-/-</sup>), MC2H (*vps28*<sup>-/-</sup>), MC4H (*vps32*<sup>-/-</sup>), MC5 (*vps28*<sup>-/-</sup>+*VPS28*), MC6 (*vps32*<sup>-/-</sup>+*VPS32*), MC13 (*rim101*<sup>-/-</sup>+*RIM101SL*), MC14 (*vps28*<sup>-/-</sup>+*RIM101SL*), and MC15 (*vps32*<sup>-/-</sup>+*RIM101SL*). Droplets of two dilutions (10<sup>5</sup> and 10<sup>4</sup> cells/ml) were spotted on SC medium (pH 5.3) and SC medium buffered at pHs 3.0, 9.0, and 10.0. Plates were incubated at 30°C for 48 h except for the plate at pH 10.0, which was incubated for 5 days.

The Rim pathway is required in *C. albicans* on several media for hypha formation, which normally occurs only at neutral and/or alkaline pH (9). Recently, several *vps* mutants were shown to affect hypha formation in *C. albicans* at alkaline pH, and these effects were partially relieved by expressing a Rim101p constitutively active form (39). To confirm the role of the ESCRT complexes in the Rim-dependent induced filamentation, we compared the *vps* mutants to the *rim101* mutant for filamentation at pH 4.0 and pH 7.5.

After 4 h at 37°C in M199 at pH 4.0, cells of all strains were in the yeast form, as were those of the reference strain (Fig. 6A), except for the *RIM101SL* suppressed strains (see below). At pH 7.5, the reference strain showed an average of 92% ± 2% of the cells producing hyphae (Fig. 6E). All deleted *rim101*<sup>-/-</sup>, *vps28*<sup>-/-</sup>, and *vps32*<sup>-/-</sup> strains were defective in filamentation, showing <5% hyphae (Fig. 6F to H) even after 36 h of incubation (data not shown). This filamentation defect was totally suppressed in the *vps28*<sup>-/-</sup>+*VPS28* and *vps32*<sup>-/-</sup>+*VPS32* complemented strains, which exhibited 92% ± 2% and 89% ± 3% of hyphal cells, respectively (Fig. 6I and J).

The introduction of the *RIM101SL* allele into the *rim101*<sup>-/-</sup>, *vps28*<sup>-/-</sup>, and *vps32*<sup>-/-</sup> mutants restored complete hypha production at pH 7.5 in 91% ± 4%, 92% ± 2%, and 92% ± 5% of the cells, respectively (Fig. 6K to M). Filamentation was also induced in these three strains at pH 4.0 with averages of 62% ± 3%, 66% ± 4%, and 76% ± 4% of the cells with hyphae, respectively (Fig. 6B to D).

These results indicate that in *C. albicans*, both *VPS28* and *VPS32* are required for alkaline-induced Rim101p-dependent hypha formation and that the 415-residue truncated form of *RIM101* induces filamentation under both acidic and alkaline conditions. Since the *VPS* deleted strains suppressed by the *RIM101SL* carry both the wild-type and the truncated alleles at the *RIM101* locus, the *RIM101SL* truncated allele appears at least partially dominant.

**Deletions in *VPS28* and *VPS32* affect virulence, kidney fungal burden, and morphogenesis in vivo.** To determine whether the MVB pathway plays a role in *C. albicans* virulence, we analyzed the *vps28*<sup>-/-</sup> and *vps32*<sup>-/-</sup> mutants in the hematogenously disseminated candidiasis model (32). Reference and isogenic strains *rim101*<sup>-/-</sup>, *vps28*<sup>-/-</sup> and *vps32*<sup>-/-</sup>, as well as complemented strains (*vps28*<sup>-/-</sup>+*VPS28* and *vps32*<sup>-/-</sup>+*VPS32*), were injected into the tail veins of mice at a dose of 2 × 10<sup>6</sup> CFU/mouse. All groups were compared by the log-rank test with highly significant differences in survival time (*P* < 0.0001) (Fig. 7). As previously shown (9), the virulence of the *rim101*<sup>-/-</sup> strain was reduced compared to the reference strain (median survival time of 8 days compared to 2 days; *P* = 0.0003). The deleted strains *vps28*<sup>-/-</sup> and *vps32*<sup>-/-</sup> appeared even more attenuated than the *rim101*<sup>-/-</sup> strain, with >50% of the mice surviving 29 days after inoculation (Fig. 7) (*P* = 0.006 for *vps28*<sup>-/-</sup> and *P* = 0.0008 for *vps32*<sup>-/-</sup>, each compared to *rim101*<sup>-/-</sup>). The dramatic virulence defect of the two *vps* mutants might be related to a growth defect in vivo. We noticed, however, that the growth rate of the *vps28*<sup>-/-</sup> mutant was comparable to that of the reference strain and that the *vps32*<sup>-/-</sup> mutant showed only a slight growth defect when strains were tested on M199 or SC at 37°C and pH 7.5, a pH comparable to the physiological pH of mammalian blood (data not shown). Complementation of the mutants with the wild-type allele repaired virulence, as all mice of the complemented groups died by 6 days for *vps32*<sup>-/-</sup>+*VPS32* and 8 days for *vps28*<sup>-/-</sup>+*VPS28*, a significant difference from their respective null mutants (*P* < 0.001 for both complemented strains). The restored virulence showed by the complemented strains, particularly *vps28*<sup>-/-</sup>+*VPS28*, was not complete, suggesting a gene dosage effect on virulence, due to the restitution of a single copy of the gene (4). However, we cannot exclude the formal possibility that part of the phenotype of the *vps28*<sup>-/-</sup> mutant resulted from additional mutations in the 28-kb region surrounding *VPS28* that may have undergone homogenization during mutant construction (see above). Similar trends in virulence were observed in mice infected with 2 × 10<sup>5</sup> CFU/mouse with each of the above strains (*P* < 0.0001; data not shown).

To assess fungal burden in kidneys, mice infected with 5 × 10<sup>5</sup> CFU/mouse were sacrificed 4 days postinfection. Figure 8 shows that mice challenged by the *C. albicans* reference strain were heavily infected with a fungal burden of 5.6 log<sub>10</sub> CFU/g of kidney, whereas mice infected with the two deleted strains *vps28*<sup>-/-</sup> and *vps32*<sup>-/-</sup> had a reduced fungal burden of 4.4 and 4.1 log<sub>10</sub> CFU/g of organ, respectively (*P* < 0.05 for both strains, each compared to the reference strain). The complemented strains *vps28*<sup>-/-</sup>+*VPS28* and *vps32*<sup>-/-</sup>+*VPS32* colonized kidneys as efficiently as the reference strain (*P* > 0.05 for both strains compared to the reference strain).

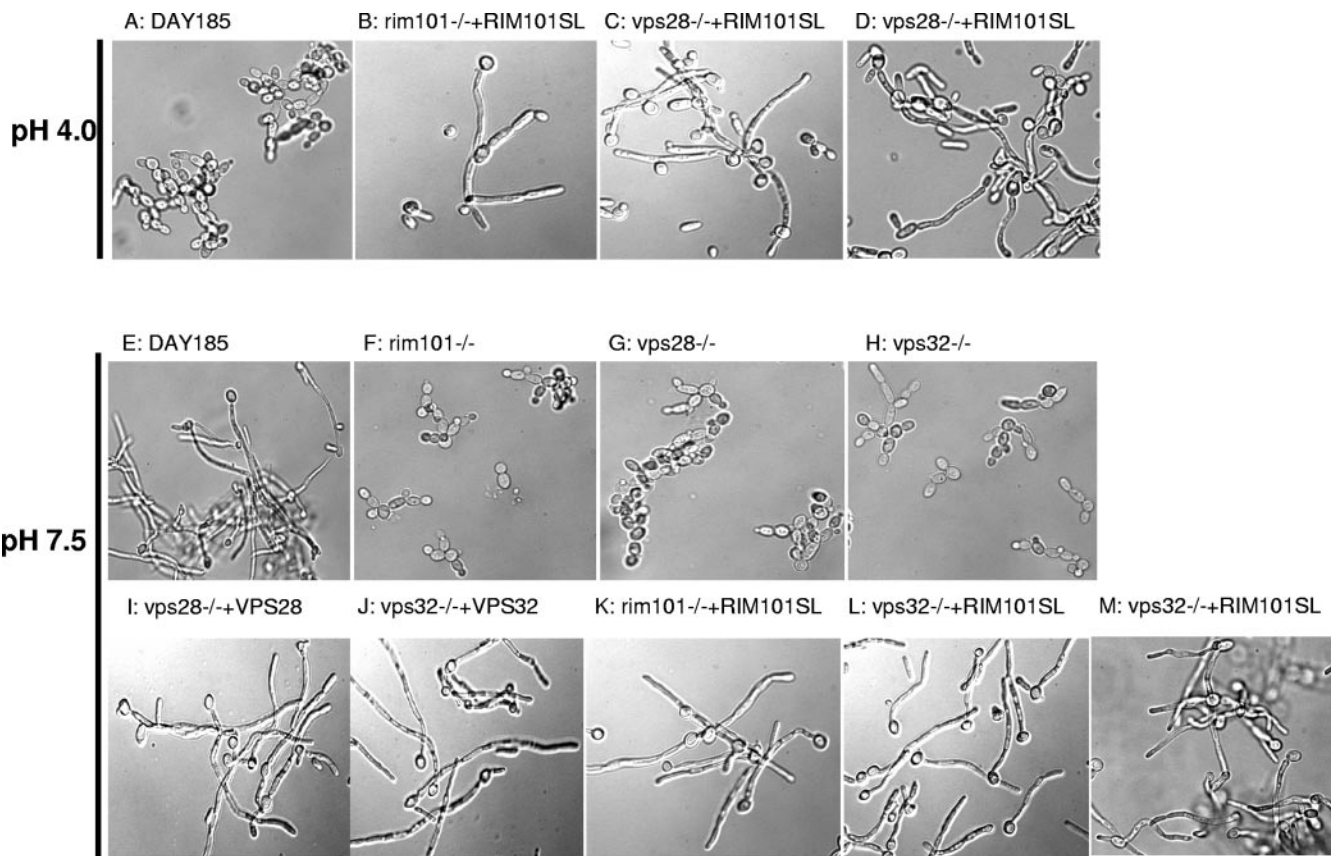


FIG. 6. Morphology of *C. albicans* cells in M199 medium adjusted to pH 4.0 or pH 7.5. The strains were DAY185 (reference strain) at pH 4.0 (A) and pH 7.5 (E); deleted strains DAY25 (*rim101*<sup>-/-</sup>), MC2H (*vps28*<sup>-/-</sup>), and MC4H (*vps32*<sup>-/-</sup>) at pH 7.5 (F to H); complemented strains MC5 (*vps28*<sup>-/-</sup>+*VPS28*) and MC6 (*vps32*<sup>-/-</sup>+*VPS32*) at pH 7.5 (I and J); and suppressed MC13 (*rim101*<sup>-/-</sup>+*RIM101SL*), MC14 (*vps28*<sup>-/-</sup>+*RIM101SL*), and MC15 (*vps32*<sup>-/-</sup>+*RIM101SL*) strains at pH 4.0 (B to D) and at pH 7.5 (K to M).

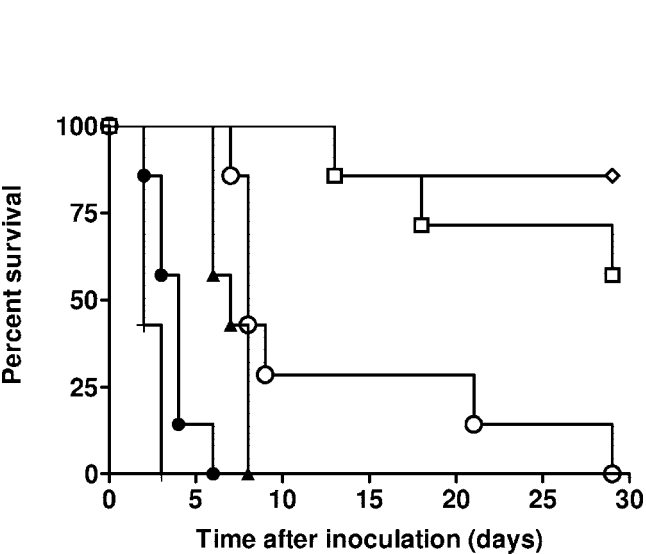


FIG. 7. Survival curves of groups of seven BALB/c male mice infected intravenously with  $2 \times 10^6$  cells of DAY185 reference strain (+); MC2H (*vps28*<sup>-/-</sup>) (□); MC4H (*vps32*<sup>-/-</sup>) (◇); MC5 (*vps28*<sup>-/-</sup>+*VPS28*) (▲); MC6 (*vps32*<sup>-/-</sup>+*VPS32*) (●); and DAY25 (*rim101*<sup>-/-</sup>) (○).

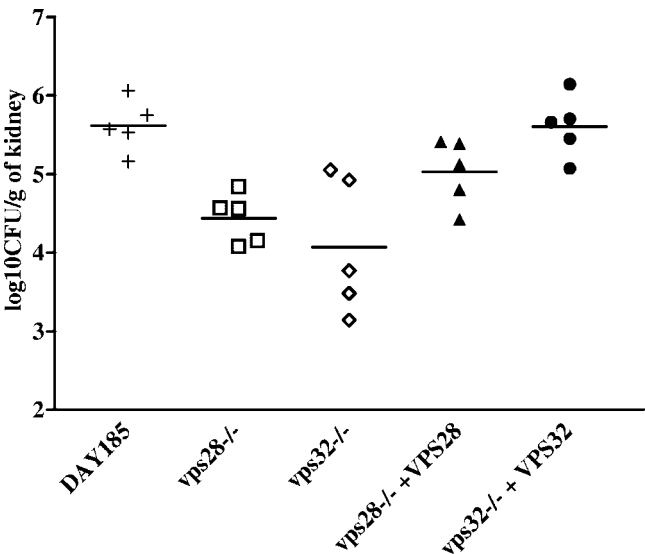


FIG. 8. Fungal burden in the kidney of BALB/c male mice infected intravenously with  $5 \times 10^5$  cells of DAY185 reference strain (+), MC2H (*vps28*<sup>-/-</sup>) (□), MC4H (*vps32*<sup>-/-</sup>) (◇), MC5 (*vps28*<sup>-/-</sup>+*VPS28*) (▲), and MC6 (*vps32*<sup>-/-</sup>+*VPS32*) (●). Each strain was inoculated in five mice.

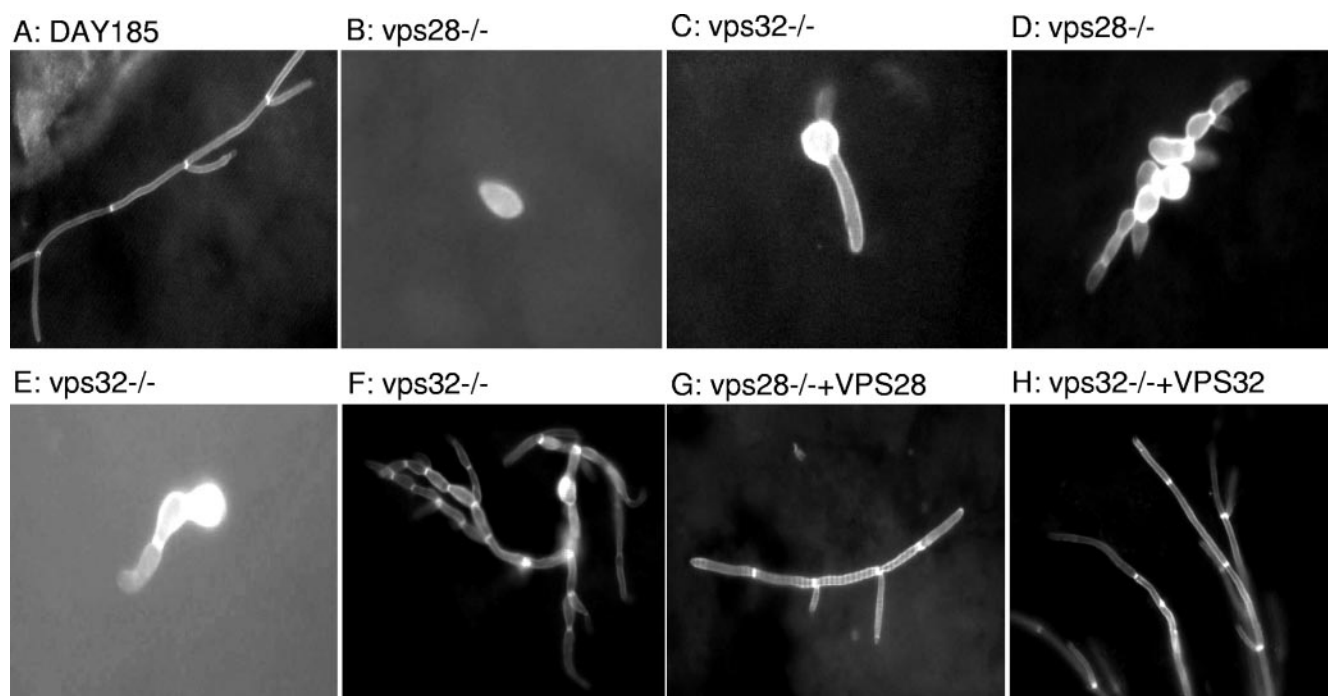


FIG. 9. Morphology of fungal elements present in the kidneys of mice infected intravenously with  $5 \times 10^5$  yeast cells of DAY185 (reference strain) (A), deleted strains MC2H (*vps28*<sup>-/-</sup>) (B and D), and MC4H (*vps32*<sup>-/-</sup>) (C, E, and F), and complemented strains MC5 (*vps28*<sup>-/-</sup> + *VPS28*) and MC6 (*vps32*<sup>-/-</sup> + *VPS32*) (G and H). Kidney homogenates obtained at day 4 postinfection were stained with 0.1% calcofluor white and 1% KOH and examined with an epifluorescence microscope.

We have shown above that the *vps*-deleted strains were defective in vitro for hyphal formation. We analyzed, by calcofluor staining, the morphology of the fungal elements present in the kidneys 4 days after infection (Fig. 9), and we used the MI to quantitate defects (Table 3). In mice infected with the reference strain, 91% of the cells had an MI score of 4, showing numerous clusters of long true hyphae (Table 3 and Fig. 9A). Conversely, only 7% and 4% of the cells had an MI score of 4 in mice infected with the *vps28*<sup>-/-</sup> and *vps32*<sup>-/-</sup> mutant strains, respectively (Table 3) ( $P < 0.01$  for both strains, each compared to the reference strain). For the mutant strains, cells were predominantly had an MI score of 3 with pseudohyphal forms (Table 3; Fig. 9D, *vps28*<sup>-/-</sup> and Fig. 9E and F, *vps32*<sup>-/-</sup>), other shapes had an MI score of 1 or 2 with yeast forms and rare germ tubes (Fig. 9B, *vps28*<sup>-/-</sup>; Fig. 9C, *vps32*<sup>-/-</sup>). Each *vps28*<sup>-/-</sup> + *VPS28* and *vps32*<sup>-/-</sup> + *VPS32* complemented strain formed comparable rates of cells with an MI score of 4, compared to the reference strain

(Table 3; Fig. 9G, *vps28*<sup>-/-</sup> + *VPS28*; Fig. 9H, *vps32*<sup>-/-</sup> + *VPS32*) ( $P > 0.05$  for both strains compared to the reference strain).

These results show that both Vps28p and Vps32p factors are required in vivo for pathogenesis. The *vps* mutants showed inadequate hyphal development and failed to colonize the kidneys as efficiently as the control strain. Such defects have already been reported for mutants of the Rim pathway (7). We demonstrate here that both *vps28* and *vps32* mutants are significantly less virulent than the *rim101* mutant, suggesting that activity of the ESCRT-I and the ESCRT-III complexes is required for virulence not only through their effect on the Rim pathway.

Such an increased effect may be related to the general role of the MWB pathway in cell physiology. The main function of this machinery in *S. cerevisiae* is to sort endosomal transmembrane proteins directed to the lumen of the vacuole away from proteins delivered to the membrane of the vacuole or to be recycled back to the plasma membrane or Golgi complex (1, 5). This control of membrane protein recycling or degradation is essential for the regulation of the cell surface composition and may thus affect various cell sensing and adaptation processes besides external pH sensing. It is thus not unexpected that defects in the MWB pathway may have a more dramatic impact than crippling the Rim pathway on cell adaptation to the extracellular environment and thus on cell survival in the host. Comparison of global changes elicited by Rim and Vps mutations may shed light on these additional processes.

#### ACKNOWLEDGMENTS

This work was supported by the Direction de la Recherche Clinique of the Assistance Publique-Hôpitaux de Paris, the Centre National de

TABLE 3. Morphology of the cells recovered from the kidneys of the mice infected intravenously with  $5 \times 10^5$  cells

Strain	Morphological form (% $\pm$ SD) of:			
	Yeasts (MI <sup>a</sup> = 1)	Elongated yeasts (MI = 2)	Pseudohyphae (MI = 3)	True hyphae (MI = 4)
DAY185	0	4 $\pm$ 3	6 $\pm$ 2	91 $\pm$ 4
<i>vps28</i> <sup>-/-</sup>	18 $\pm$ 4	24 $\pm$ 12	51 $\pm$ 8	7 $\pm$ 4
<i>vps32</i> <sup>-/-</sup>	10 $\pm$ 6	22 $\pm$ 9	64 $\pm$ 15	4 $\pm$ 5
<i>vps28</i> <sup>-/-</sup> + <i>VPS28</i>	1 $\pm$ 1	1 $\pm$ 1	6 $\pm$ 2	92 $\pm$ 3
<i>vps32</i> <sup>-/-</sup> + <i>VPS32</i>	1 $\pm$ 1	2 $\pm$ 2	7 $\pm$ 3	90 $\pm$ 5

<sup>a</sup> MI, morphological index score (27).

la Recherche Scientifique, and grants from Merck & Company and Fujisawa, Inc., through funding of M.C.; and by the European Commission (QLK2-2000-00795, Galar Fungail Consortium), through funding of F.B.

Sequence data from *C. albicans* were obtained from the Stanford DNA Sequencing and Technology Center, with the support of the NIDR and the Burroughs Wellcome Fund.

Plasmids carrying the *MET3* promoter (pFLAG-MET3) were kindly donated by Y. Uehara, and strains deleted for *RIM101*, BWP17, pDDB78, and UAU1-carrying plasmids were a generous gift from A. P. Mitchell. Helpful discussions with members of the lab, particularly Mathias Richard, are greatly acknowledged.

#### REFERENCES

- Babst, M. 2005. A protein's final ESCRT. *Traffic* 6:2–9.
- Babst, M., D. J. Katzmman, E. J. Estepa-Sabal, T. Meerloo, and S. D. Emr. 2002. Escrt-III: an endosome-associated heterooligomeric protein complex required for mvb sorting. *Dev. Cell* 3:271–282.
- Babst, M., B. Wendland, E. J. Estepa, and S. D. Emr. 1998. The Vps4p AAA ATPase regulates membrane association of a Vps protein complex required for normal endosome function. *EMBO J.* 17:2982–2993.
- Bates, S., D. M. MacCallum, G. Bertram, C. A. Munro, H. B. Hughes, E. T. Buurman, A. J. Brown, F. C. Odds, and N. A. Gow. 2005. *Candida albicans* Pmr1p, a secretory pathway P-type  $\text{Ca}^{2+}/\text{Mn}^{2+}$ -ATPase, is required for glycosylation and virulence. *J. Biol. Chem.* 280:23408–23415.
- Bignell, E., S. Negrete-Urtasun, A. M. Calcagno, K. Haynes, H. N. Arst, Jr., and T. Rogers. 2005. The *Aspergillus* pH-responsive transcription factor PacC regulates virulence. *Mol. Microbiol.* 55:1072–1084.
- Bowers, K., J. Lottridge, S. B. Helliwell, L. M. Goldthwaite, J. P. Luzio, and T. H. Stevens. 2004. Protein-protein interactions of ESCRT complexes in the yeast *Saccharomyces cerevisiae*. *Traffic* 5:194–210.
- Calderone, R. A., and W. A. Fonzi. 2001. Virulence factors of *Candida albicans*. *Trends Microbiol.* 9:327–335.
- Davis, D. 2003. Adaptation to environmental pH in *Candida albicans* and its relation to pathogenesis. *Curr. Genet.* 44:1–7.
- Davis, D., J. E. Edwards, Jr., A. P. Mitchell, and A. S. Ibrahim. 2000. *Candida albicans* RIM101 pH response pathway is required for host-pathogen interactions. *Infect. Immun.* 68:5953–5959.
- Davis, D., R. B. Wilson, and A. P. Mitchell. 2000. RIM101-dependent and-independent pathways govern pH responses in *Candida albicans*. *Mol. Cell Biol.* 20:971–978.
- De Bernardis, F., F. A. Muhlschlegel, A. Cassone, and W. A. Fonzi. 1998. The pH of the host niche controls gene expression in and virulence of *Candida albicans*. *Infect. Immun.* 66:3317–3325.
- Eggimann, P., J. Garbino, and D. Pittet. 2003. Management of *Candida* species infections in critically ill patients. *Lancet Infect. Dis.* 3:772–785.
- El Barkani, A., O. Kurzai, W. A. Fonzi, A. Ramon, A. Porta, M. Frosch, and F. A. Muhlschlegel. 2000. Dominant active alleles of RIM101 (PRR2) bypass the pH restriction on filamentation of *Candida albicans*. *Mol. Cell Biol.* 20:4635–4647.
- Enloe, B., A. Diamond, and A. P. Mitchell. 2000. A single-transformation gene function test in diploid *Candida albicans*. *J. Bacteriol.* 182:5730–5736.
- Espeso, E. A., J. Tilburn, L. Sanchez-Pulido, C. V. Brown, A. Valencia, H. N. Arst, Jr., and M. A. Penalva. 1997. Specific DNA recognition by the *Aspergillus nidulans* three zinc finger transcription factor PacC. *J. Mol. Biol.* 274:466–480.
- Fonzi, W. A. 1999. PHR1 and PHR2 of *Candida albicans* encode putative glycosidases required for proper cross-linking of  $\beta$ -1,3- and  $\beta$ -1,6-glucans. *J. Bacteriol.* 181:7070–7079.
- Fonzi, W. A. 2002. Role of pH response in *Candida albicans* virulence. *Mycoses* 45(Suppl. 1):16–21.
- Gavin, A. C., M. Bosche, R. Krause, P. Grandi, M. Marzioch, A. Bauer, J. Schultz, J. M. Rick, A. M. Michon, C. M. Cruciat, M. Remor, C. Hofert, M. Schelder, M. Brajenovic, H. Ruffner, A. Merino, K. Klein, M. Hudak, D. Dickson, T. Rudi, V. Gnau, A. Bauch, S. Bastuck, B. Huhse, C. Leutwein, M. A. Heurtier, R. R. Copley, A. Edelmann, E. Querfurth, V. Rybin, G. Drewes, M. Raida, T. Bouwmeester, P. Bork, B. Seraphin, B. Kuster, G. Neubauer, and G. Superti-Furga. 2002. Functional organization of the yeast proteome by systematic analysis of protein complexes. *Nature* 415:141–147.
- Ghannoum, M. A., B. Spellberg, S. M. Saporito-Irwin, and W. A. Fonzi. 1995. Reduced virulence of *Candida albicans* PHR1 mutants. *Infect. Immun.* 63:4528–4530.
- Gonzalez-Lopez, C. I., R. Szabo, S. Blanchin-Roland, and C. Gaillardin. 2002. Genetic control of extracellular protease synthesis in the yeast *Yarrowia lipolytica*. *Genetics* 160:417–427.
- Ito, T., T. Chiba, R. Ozawa, M. Yoshida, M. Hattori, and Y. Sakaki. 2001. A comprehensive two-hybrid analysis to explore the yeast protein interactome. *Proc. Natl. Acad. Sci. USA* 98:4569–4574.
- Katzmann, D. J., M. Babst, and S. D. Emr. 2001. Ubiquitin-dependent sorting into the multivesicular body pathway requires the function of a conserved endosomal protein sorting complex, ESCRT-I. *Cell* 106:145–155.
- Katzmann, D. J., G. Odorizzi, and S. D. Emr. 2002. Receptor downregulation and multivesicular-body sorting. *Nat. Rev. Mol. Cell Biol.* 3:893–905.
- Kullas, A. L., M. Li, and D. A. Davis. 2004. Snf7p, a component of the ESCRT-III protein complex, is an upstream member of the RIM101 pathway in *Candida albicans*. *Eukaryot. Cell* 3:1609–1618.
- Lambert, M., S. Blanchin-Roland, F. Le Louedec, A. Lepingle, and C. Gaillardin. 1997. Genetic analysis of regulatory mutants affecting synthesis of extracellular proteinases in the yeast *Yarrowia lipolytica*: identification of a RIM101/pacC homolog. *Mol. Cell Biol.* 17:3966–3976.
- Li, M., S. J. Martin, V. M. Bruno, A. P. Mitchell, and D. A. Davis. 2004. *Candida albicans* Rim13p, a protease required for Rim101p processing at acidic and alkaline pHs. *Eukaryot. Cell* 3:741–751.
- Odds, F. C., L. Van Nuffel, and N. A. Gow. 2000. Survival in experimental *Candida albicans* infections depends on inoculum growth conditions as well as animal host. *Microbiology* 146:1881–1889.
- Odorizzi, G., D. J. Katzmman, M. Babst, A. Audhya, and S. D. Emr. 2003. Bro1 is an endosome-associated protein that functions in the MVB pathway in *Saccharomyces cerevisiae*. *J. Cell Sci.* 116:1893–1903.
- Penalva, M. A., and H. N. Arst, Jr. 2004. Recent advances in the characterization of ambient pH regulation of gene expression in filamentous fungi and yeasts. *Annu. Rev. Microbiol.* 58:425–451.
- Porta, A., A. M. Ramon, and W. A. Fonzi. 1999. *PRR1*, a homolog of *Aspergillus nidulans* *palF*, controls pH-dependent gene expression and filamentation in *Candida albicans*. *J. Bacteriol.* 181:7516–7523.
- Ramon, A. M., A. Porta, and W. A. Fonzi. 1999. Effect of environmental pH on morphological development of *Candida albicans* is mediated via the PacC-related transcription factor encoded by *PRR2*. *J. Bacteriol.* 181:7524–7530.
- Richard, M., S. Ibata-Ombetta, F. Dromer, F. Bordon-Pallier, T. Jouault, and C. Gaillardin. 2002. Complete glycosylphosphatidylinositol anchors are required in *Candida albicans* for full morphogenesis, virulence and resistance to macrophages. *Mol. Microbiol.* 44:841–853.
- Rieder, S. E., L. M. Banta, K. Kohrer, J. M. McCaffery, and S. D. Emr. 1996. Multilamellar endosome-like compartment accumulates in the yeast vps28 vacuolar protein sorting mutant. *Mol. Biol. Cell* 7:985–999.
- Saporito-Irwin, S. M., C. E. Birse, P. S. Sypherd, and W. A. Fonzi. 1995. PHR1, a pH-regulated gene of *Candida albicans*, is required for morphogenesis. *Mol. Cell Biol.* 15:601–613.
- Tilburn, J., S. Sarkar, D. A. Widdick, E. A. Espeso, M. Orejas, J. Mungroo, M. A. Penalva, and H. N. Arst, Jr. 1995. The *Aspergillus* PacC zinc finger transcription factor mediates regulation of both acid- and alkaline-expressed genes by ambient pH. *EMBO J.* 14:779–790.
- Umeyama, T., Y. Nagai, M. Niimi, and Y. Uehara. 2002. Construction of FLAG tagging vectors for *Candida albicans*. *Yeast* 19:611–618.
- Vida, T. A., and S. D. Emr. 1995. A new vital stain for visualizing vacuolar membrane dynamics and endocytosis in yeast. *J. Cell Biol.* 128:779–792.
- Wilson, R. B., D. Davis, and A. P. Mitchell. 1999. Rapid hypothesis testing with *Candida albicans* through gene disruption with short homology regions. *J. Bacteriol.* 181:1868–1874.
- Xu, W., F. J. Smith, Jr., R. Subaran, and A. P. Mitchell. 2004. Multivesicular body-ESCRT components function in pH response regulation in *Saccharomyces cerevisiae* and *Candida albicans*. *Mol. Biol. Cell* 15:5528–5537.